

Oridonin induces apoptosis in oral squamous cell carcinoma probably through the generation of reactive oxygen species and the p38/JNK MAPK pathway

HA-NA OH^{1*}, JI-HYE SEO^{2*}, MEE-HYUN LEE³, GOO YOON¹, SEUNG-SIK CHO¹, KANGDONG LIU^{3,4}, HYUNJI CHOI⁵, KEON BONG OH⁶, YOUNG-SIK CHO⁷, HANGUN KIM⁸, ALUM HAN⁹, JUNG-IL CHAE² and JUNG-HYUN SHIM^{1,3}

¹Department of Pharmacy, College of Pharmacy and Natural Medicine Research Institute, Mokpo National University, Jeonnam 58554; ²Department of Dental Pharmacology, School of Dentistry and Institute of Oral Bioscience, BK21 Plus, Chonbuk National University, Jeonju 54896, Republic of Korea; ³The China-US (Henan) Hormel Cancer Institute, Zhengzhou, Henan 450008; ⁴School of Basic Medical Sciences, Zhengzhou University, Zhengzhou, Henan 450001, P.R. China; ⁵Department of Biological Sciences, Dong-A University, Busan 49315; ⁶Animal Biotechnology Division, National Institute of Animal Science, RDA, Wanju 55365; ⁷Department of Pharmacy, Keimyung University, Daegu 42601; ⁸College of Pharmacy and Research Institute of Life and Pharmaceutical Sciences, Sunchon National University, Sunchon 57922; ⁹Department of Family Medicine, Medical Hospital, Wonkwang University, Iksan, Chonbuk 54538, Republic of Korea

Received November 16, 2017; Accepted March 14, 2018

DOI: 10.3892/ijo.2018.4319

Abstract. The anti-inflammatory effects of oridonin (Ordn) have been well established in previous studies. However, the apoptotic effects of Ordn on oral cancer cells have not yet

been evaluated, at least to the best of our knowledge. The aim of this study was to examine the apoptotic activity of Ordn in oral squamous cell carcinoma cells and to elucidate the underlying mechanisms. For this purpose, we employed experimental techniques, such as MTT assay, DAPI staining, soft agar assay, flow cytometry and western blot analysis. Our results revealed that Ordn suppressed oral cancer cell proliferation and soft agar colony formation, while it induced reactive oxygen species (ROS)-dependent apoptosis in a dose or time-dependent manner. The generation of ROS was detected in HN22 and HSC4 cells treated with Ordn and the use of the free radical scavenger, N-acetyl-L-cysteine, almost blocked Ordn-induced apoptosis. The phosphorylation of JNK and p38 mitogen-activated protein kinase (MAPK) was manifested in the Ordn-treated cells. Furthermore, Ordn induced the apoptosis of oral cancer cells through the mitochondrial-dependent pathway, involving the loss of mitochondrial membrane potential, the release of cytochrome *c*, the induction of poly(ADP-Ribose) polymerase (PARP) cleavage, alterations in the ratios of apoptotic proteins and the activation of the caspase cascade. Taken together, these findings indicate that Ordn induces the apoptosis of oral cancer cells probably via ROS-mediated JNK/p38 MAPK and mitochondrial pathways; thus, Ordn may have potential for use in the treatment of oral cancer.

Correspondence to: Professor Jung-Hyun Shim, Department of Pharmacy, College of Pharmacy and Natural Medicine Research Institute, Mokpo National University, Mu-an-gun, 1666 Yeongsan-ro, Jeonnam 58554, Republic of Korea
E-mail: sl004jh@gmail.com

Professor Jung-Il Chae, Department of Dental Pharmacology, School of Dentistry, BK21 Plus, Chonbuk National University, 567 Baekje-daero, Jeonju 54896, Republic of Korea
E-mail: jichae@jbnu.ac.kr

*Contributed equally

Abbreviations: OSCC, oral squamous cell carcinoma; Ordn, oridonin; ROS, reactive oxygen species; DR, death receptor; MAPK, mitogen-activated protein kinase; ERKs, extracellular signal-related kinases; JNKs, c-jun NH2-terminal kinases; FBS, fetal bovine serum; PBS, phosphate-buffered saline; NAC, N-acetyl-L-cysteine; MTT, 3-(4,5-dimethylthiazol-2-yl)-2,5 diphenyltetrazolium bromide; MMP, mitochondrial membrane potential; 7-AAD, 7-aminoactinomycin D; DAPI, 4'-6-diamidino-2-phenylindole; CHOP, CCAAT/enhancer-binding protein homologous protein; Mcl-1, myeloid cell leukemia-1; tBid, truncated Bid; Apaf-1, apoptotic protease activating factor-1; cyto *c*, cytochrome *c*; PARP, poly(ADP-Ribose) polymerase

Key words: oridonin, oral cancer, apoptosis, reactive oxygen species, p38, c-jun NH2-terminal kinase

Introduction

Oral cancer is a rare disease accounting for <5% of all malignancies worldwide (1). Despite the fact that it is a rare type of cancer, it has been shown that oral cancer is associated with the use of smokeless tobacco in middle-aged

individuals >40 years of age (2). The disruption of normal cell function by smoking and alcohol consumption can cause oral cancer, and moreover, there is a synergistic effect if smoking and drinking are used simultaneously (2). Oral cancer includes squamous epidermal carcinoma, adenoid cystic carcinoma, mucoepidermoid carcinoma and adenocarcinoma. Among these, the main type of oral cancer is squamous cell carcinoma (3). The prognosis of oral cancer varies widely depending on the tumor-node-metastasis staging system (4). If oral cancer is detected in its earliest stage, the majority of patients have a high 5-year survival rate (5). The therapeutic strategies against oral cancer include surgery, radiation and chemo-radiotherapy (4). Some anticancer drugs used in oral cancer are highly toxic and inefficient (6). The toxicity of these drugs in normal cells has been one of the major obstacles to successful cancer chemotherapy (6). Additionally, oral cancer still has oral cancer-specific target molecules that have not yet been discovered, despite the suggestion of promising targets, such as cyclooxygenase and epidermal growth factor receptor, as well as others (7). With the further identification of target proteins, extensive research and the development of specific tumor biomarkers are warranted for the effective treatment of oral cancer.

It has been reported that there are many natural products with anticancer effects (6,8). Among these, oridonin (Ordn) is a bioactive ent-kaurene diterpenoid found in *Rabdosia rubescens* (9). *Rabdosia rubescens* is also known as Dong Ling Cao in traditional Chinese medicine, and has been used in the treatment of stomach aches, pharyngitis, sore throats and coughs (8). A recent study indicated that Ordn exerts potent antioxidant, anti-bacterial, anti-inflammatory, pro-apoptotic, anticancer and neurological effects (10). In addition, *Rabdosia rubescens* has long been used in China due to its low toxicity and lack of side-effects (11). However, it has not yet been proven whether or not Ordn can be effectively used in the treatment of cancer.

Reactive oxygen species (ROS) are by-products of normal cellular metabolism during respiration process or organic compounds and can be beneficial or harmful to cells, depending on their concentrations (12). A marked increase in ROS levels can cause oxidative stress and can induce cell death, including apoptosis, autophagy and necrosis (13). When cells are exposed to ROS-induced stress, the mitogen-activated protein kinase (MAPK) cascade is sequentially activated, mainly including growth factor-regulated extracellular signal-related kinases (ERKs), c-jun NH2-terminal kinases (JNKs) and p38 MAPKs (14). It has been demonstrated that apoptosis induced by ROS is mediated by p38 and JNK activation (15). MAPKs play an important role in the regulation of cellular processes, such as cell growth and proliferation, differentiation and apoptosis (16).

Apoptosis is an important phenomenon in cell death induced by anticancer drugs and contributes to the elimination of unnecessary and unwanted cells via macrophages and neighboring cells (17). Programmed cell death is associated with characteristic morphological and biochemical events (18). Endoplasmic reticulum (ER) stress can activate specific apoptotic pathways to eliminate severely damaged cells, in which protein folding defects cannot be resolved (19). Various ER stress inducers have consistently been shown to induce CCAAT/enhancer-binding

protein homologous protein (CHOP), and death receptor (DR)4 and DR5 expression on cell surfaces (20). Under the apoptotic cascade, the collapse of mitochondrial membrane potential (MMP) is a prominent hallmark, indicating that the mitochondrial apoptotic pathway is consequently activated (21). Anticancer drugs may disrupt the mitochondria by increasing the permeability of the outer mitochondrial membrane that may result in the obstruction of intracellular ATP synthesis, and the release of cytochrome *c* (cyto *c*) to the cytosol to form apoptosomes and to boost a series of caspases (22). The ability of the mitochondria to mediate apoptosis is tightly regulated by various related proteins (23). As a result, specific pro-apoptotic/anti-apoptotic proteins, such as p21, p27, myeloid cell leukemia-1 (Mcl-1), survivin, truncated Bid (tBid) and Bax can potentially determine the response of cancer cells to the apoptotic signal (24,25).

However, whether or not Ordn exerts pro-apoptotic effects probably through the modulation of the p38 and JNK signaling pathways remains unclear. Therefore, the aim of the present study was to investigate the antitumor effects of Ordn on the oral cancer cell lines, HN22 and HSC4 cells, and to further elucidate the molecular mechanism involved in its anti-neoplastic activities.

Materials and methods

Reagents and antibodies. Ordn (chemical structure shown in Fig. 1A) was kindly provided by professor Zigang Dong of China-US (Henan) Hormel Cancer Institute (Zhengzhou, Henan, China). Dulbecco's modified Eagle's medium, fetal bovine serum (FBS), trypsin, penicillin and streptomycin and phosphate-buffered saline (PBS) were purchased from HyClone (Logan, UT, USA). Antibodies against CHOP (sc-793), DR4 (sc-7863), DR5 (sc-166624), poly(ADP-Ribose) polymerase (PARP)-1 (sc-7150), p21 (sc-6246), p27 (sc-528), Mcl-1 (sc-819), survivin (sc-17779), Bax (sc-493), cyto *c* (sc-13156), α -tubulin (sc-5286), cytochrome *c* oxidase 4 (COX4; sc-69359), apoptotic protease activating factor-1 (Apaf-1; sc-33870) and actin (sc-1615) were purchased from Santa Cruz Biotechnology, Inc. (Santa Cruz, CA, USA). The specific antibodies to JNK (#9252), p-JNK (Thr183/Tyr185; #9251), p38 (#9212), p-p38 (Thr180/Tyr182; #9211) and tBid (#2002) were obtained from Cell Signaling Technologies (Danvers, MA, USA). Basal Medium Eagle, 4',6-diamidino-2-phenylindole (DAPI), N-acetyl-L-cysteine (NAC) and 3-(4,5-dimethylthiazol-2-yl)-2,5-diphenyltetrazolium bromide (MTT) were obtained from Sigma-Aldrich, Inc. (St. Louis, MO, USA).

Cell culture. The HN22 (RRID:CVCL_5522) cell line has been described previously (26), and was provided by Dankook University (Cheonan, Korea). The HSC4 (RRID:CVCL_1289) cell line was obtained from the Human Science Research Resources Bank (Osaka, Japan), and was provided by Hokkaido University (Hokkaido, Japan). The cells were maintained in Dulbecco's modified Eagle's medium containing 10% heat-inactivated FBS and 100 U/ml each of penicillin and streptomycin at 37°C in a 5% CO₂ incubator.

MTT assay. The HN22 (2 x 10³/well) and HSC4 (2.5 x 10³/well) cells were seeded into 96-well plates. Following incubation

overnight, the adherent cells were exposed to various concentrations (0, 5, 7.5 and 10 μ M) of Ord n for 24 and 48 h. Following treatment, 30 μ l of MTT solution (5 mg/ml) were added to each well followed by incubation for a further 2 h at 37°C. The supernatant was subsequently removed and DMSO was then added to the cells. To solubilize the formazan, the 96-well plates were gently mixed on a gyratory shaker for 5 min at 37°C. The absorbance of the formazan solution was recorded at a wavelength of 570 nm by Enspire Multimode Plate reader (Perkin-Elmer, Akron, OH, USA). The viability results are expressed as the IC₅₀ mean values of 3 independent experiments.

Anchorage-independent cell transformation assay. The oral cancer cells suspended in Basal Medium Eagle supplemented with FBS, gentamicin and L-glutamine were added to 0.3% agar in a top layer over a base layer of 0.6% agar containing Ord n (1, 2 and 4 μ M). The cultures were maintained at 37°C in a 5% CO₂ incubator for 3 weeks, and then the cell colonies were counted under a microscope (Olympus Corporation, Tokyo, Japan).

DAPI staining. The number of cells undergoing apoptosis was quantified after DAPI staining. Briefly, the HN22 and HSC4 cells were treated with Ord n (5, 7.5 and 10 μ M) for 48 h and then harvested by trypsinization. The cells were washed a third time with PBS and centrifuged at 850 x g for 5 min at 4°C. The cell pellets were fixed in 100% methanol at room temperature for 30 min. The cells were deposited on slides and stained with DAPI solution in the dark. Subsequently, the DAPI-stained apoptotic cells were observed under an Olympus IX79-DP73 fluorescence microscope (Olympus Corporation).

Cell cycle analysis. The assay was performed using the Muse™ Cell Cycle kit (MCH100106; Merck Millipore, Billerica, MA, USA) to measure the DNA content at cell cycle stages (G0/G1, S and G2/M), as previously described (27). Either the HN22 or the HSC4 cells were plated in a 6-well plate and treated with Ord n at various concentrations (0, 5, 7.5 and 10 μ M) for 48 h at 37°C. The cells were harvested and then suspended in cold PBS. The cell pellets were fixed in cold 70% ethanol for overnight at -20°C. After washing again with cold PBS, the cells were stained with Muse™ Cell Cycle kit reagent. Following 30 min of incubation at room temperature in the dark, the cell cycle distribution was analyzed using the Muse™ cell analyzer flow cytometer (Merck Millipore).

Annexin V staining. According to the manufacturer's instructions, the assay was carried out using the Muse™ Annexin V and Dead Cell kit (MCH100105; Merck Millipore). Briefly, the HN22 and HSC4 cells were seeded in a 6-well plate and incubated at 37°C for 24 h. The cells were treated with Ord n (0, 5, 7.5 and 10 μ M), harvested, washed twice with cold PBS and transferred to 1.5 ml microcentrifuge tubes. Muse™ Annexin V and Dead Cell reagent was then added to each tube, followed by incubation for a further 20 min at room temperature in the dark. The analyses of apoptotic cells were carried out using the Muse™ cell analyzer.

Determination of ROS levels. The assay was performed using the Muse™ cell Analyzer to determine oxidative stress induced

by Ord n. The Muse™ Oxidative Stress Kit (MCH100111; Merck Millipore) allows for the quantitative measurements of ROS levels in cells subjected to oxidative stress. Following treatment with Ord n (0, 5, 7.5 and 10 μ M), the HN22 and HSC4 cells were collected. Following centrifugation (1,500 g, 5 min, room temperature), the cells were resuspended in 1X assay buffer. Finally, 190 μ l of Muse™ Oxidative Stress working solution was mixed with 10 μ l of the cell suspension and incubated at 37°C for 30 min prior to analysis. Following incubation, the stained cells were examined using the Muse™ cell analyzer.

Measurement of MMP. To examine the changes in mitochondrial transmembrane potential at the early stages, MMP was measured using the Muse™ Cell Analyzer with the Muse MitoPotential Assay kit (MCH100110; Merck Millipore). The HN22 and HSC4 cells were seeded on 6-well plates for 24 h and then treated with various concentrations (0, 5, 7.5 and 10 μ M) of Ord n for 48 h. The harvested cells were washed with PBS and collected by centrifugation at 1,500 x g for 5 min at room temperature. Following centrifugation, the supernatant was removed and the cell pellets were stained with the Muse™ MitoPotential working solution for 20 min at 37°C. After the cells were stained with 7-aminoactinomycin D (7-AAD) for 5 min at room temperature, the stained cells were examined using the Muse™ cell analyzer.

Multi-caspase assay. The assay was carried out using the Muse™ Multi-caspase assay kit (MCH100109; Merck Millipore) to assess the activation of multiple caspases (caspase-1, -3, -4, -5, -6, -7, -8 and -9). Briefly, HN22 and HSC4 cells were seeded at 37°C in a 6-well plate for 24 h. After treatment with various doses of Ord n (0, 5, 7.5 and 10 μ M), the cells were washed in PBS and resuspended in 1X caspase buffer. Muse™ Multi-Caspase reagent working solution was added to the cells and kept incubated for 30 min at 37°C. One hundred and fifty microliters of Muse™ Caspase 7-AAD working solution was added in each tube and incubated for 5 min at room temperature. The data were analyzed using the Muse™ cell analyzer.

Western blot analysis. The cells were harvested and washed with cold PBS. Cell lysates were carried out using RIPA lysis buffer and the lysate was then subjected to centrifugation at 16,000 x g for ~30 min at 4°C. Total protein concentrations in the supernatant were determined through calibration with BSA. Total protein extracts were separated electrophoretically using 10, 12 or 15% SDS-PAGE gels and transferred onto polyvinylidene fluoride membranes. After the transfer, the membranes were blocked for ~2 h at room temperature with skim milk. The membranes incubated overnight at 4°C with antibodies (all diluted 1:1,000) against CHOP, DR4, DR5, PARP, C-PARP, p38, p-p38, JNK, p-JNK, p21, p27, Mcl-1, survivin, tBid, Bax, cyto c, COX4, α -tubulin, Apaf-1 and actin. After washing 5 times, the membranes were incubated with a horseradish peroxidase-conjugated secondary antibody [goat anti-rabbit IgG (#31460, 1:6,000 dilution), goat anti-mouse IgG (#31430, 1:5,000 dilution) (both from Thermo Fisher Scientific, Waltham, MA, USA) and donkey anti-goat IgG (sc-2020, 1:4,000 dilution; Santa Cruz Biotechnology, Inc.) for 2 h at

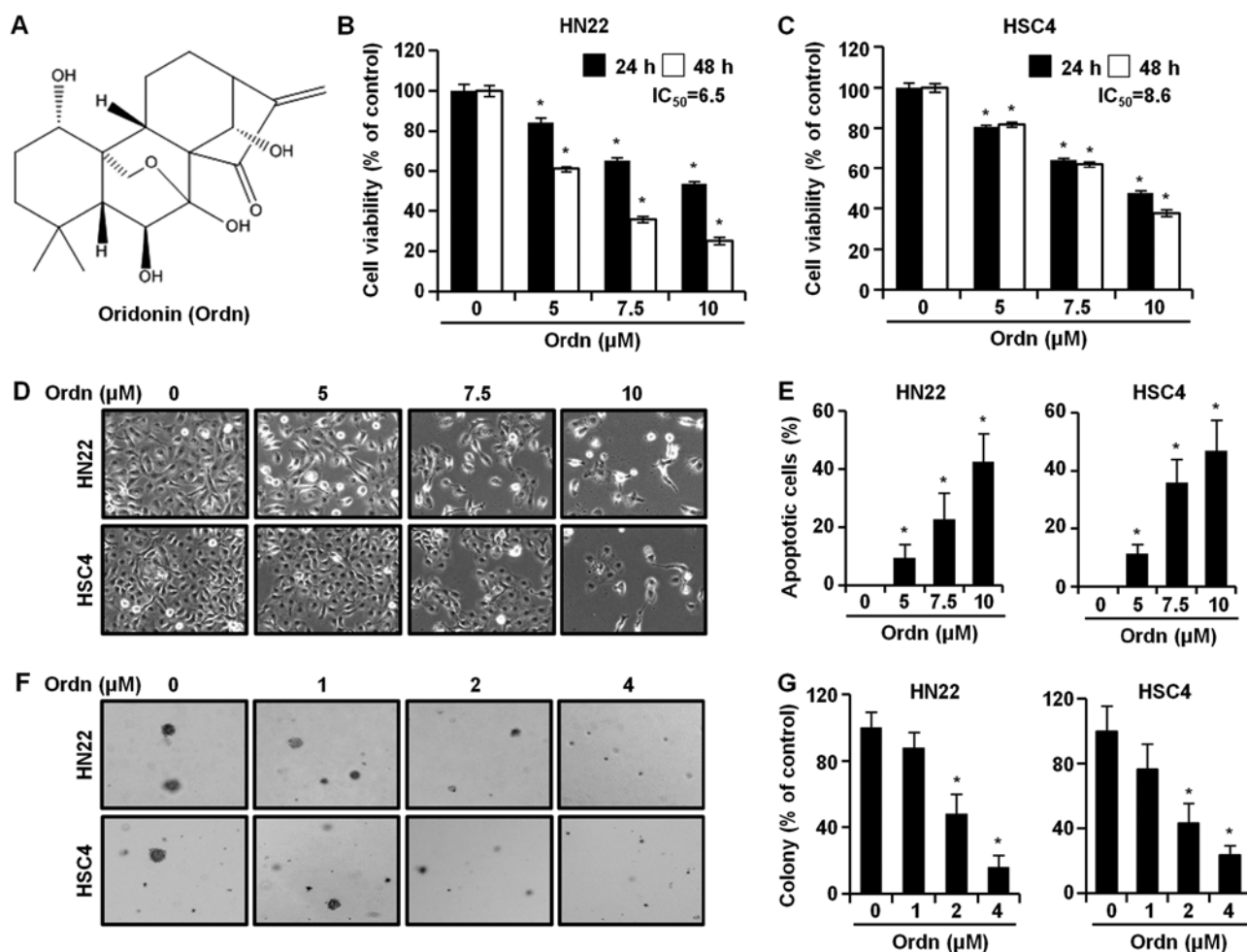


Figure 1. Effects of oridonin (Ordn) on the viability and anchorage-independent growth of HN22 and HSC4 cells. (A) Chemical structure of Ordn. (B and C) The cells were treated with Ordn (0, 5, 7.5 and 10 μ M) for 24 or 48 h. Cell viability was determined by MTT assay. The cells were treated with the indicated concentration of Ordn for 24 or 48 h. (D) Following Ordn treatment at a given concentration for 48 h, morphological changes in the HN22 and HSC4 cells were observed under an inverted light microscope. (E) The graphs indicate the quantified numbers of apoptotic DNA fragmentation and chromatin condensation after DAPI-staining. Ordn inhibited the anchorage-independent growth of (F) HN22 and (G) HSC4 cells. Cells were treated with 0, 5, 7.5, or 10 μ M Ordn for 3 weeks. The asterisks (*) indicate significant differences ($P < 0.05$) between the untreated and Ordn-treated groups. Data are representative of 3 independent experiments, each time in triplicate.

room temperature. Immunoblotting was performed using the ECL Plus Western blotting detection system (Santa Cruz Biotechnology, Inc.) and then each protein was quantified by ImageJ Instrument software.

Statistical analysis. The data are presented as the means \pm SD. Statistical analysis of the data was performed using the Prism 5.0 statistical package. The statistical significance of differences among groups were analyzed using ANOVA and Fisher's Least Significant Difference post hoc test. Mean values were considered statistically significant at $P < 0.05$. In the present study, the data are representative of 3 independent experiments in triplicate.

Results

Ordn inhibits the proliferation and colony-forming ability of oral cancer cells. To examine the effects of Ordn on the viability of the oral cancer cell lines, HN22 and HSC4, we performed MTT assay, measuring the activity of mitochondrial dehydrogenases (28). We treated the cells with Ordn for

different periods of time (24 or 48 h) and various concentrations. As a result, Ordn significantly decreased the viability of both the HN22 (Fig. 1B) and HSC4 (Fig. 1C) cells in a dose- and time-dependent manner. As shown in Fig. 1B and C, the IC_{50} values of Ordn were determined from the dose-response curves of the HN22 and HSC4 cells, accounting for 6.5 and 8.6 μM in the HN22 and HSC4 cells, respectively. Treatment of the HN22 cells with Ordn at 5, 7.5 and 10 μM for 48 h decreased cell viability to 60.97, 35.81 and 25.14% relative to that of the control, respectively. Similarly, the viability of the HSC4 cells treated with Ordn at 5, 7.5 and 10 μM for 48 h dose-dependently decreased to 81.77, 62.02 and 37.81% relative to that of the control, respectively. Morphological changes were examined under an optical microscope following treatment of the oral cancer cells with Ordn at concentrations of 0, 5, 7.5 and 10 μM for 48 h. As shown in Fig. 1D, it was found that the control cells exhibited normal cell shapes with a clear outline and were spread evenly in the culture plates. Following 48 h of treatment with Ordn, a significant proportion of the oral cancer cells became dislodged from the plates. In addition, the remaining adherent oral cancer cells exhibited typical

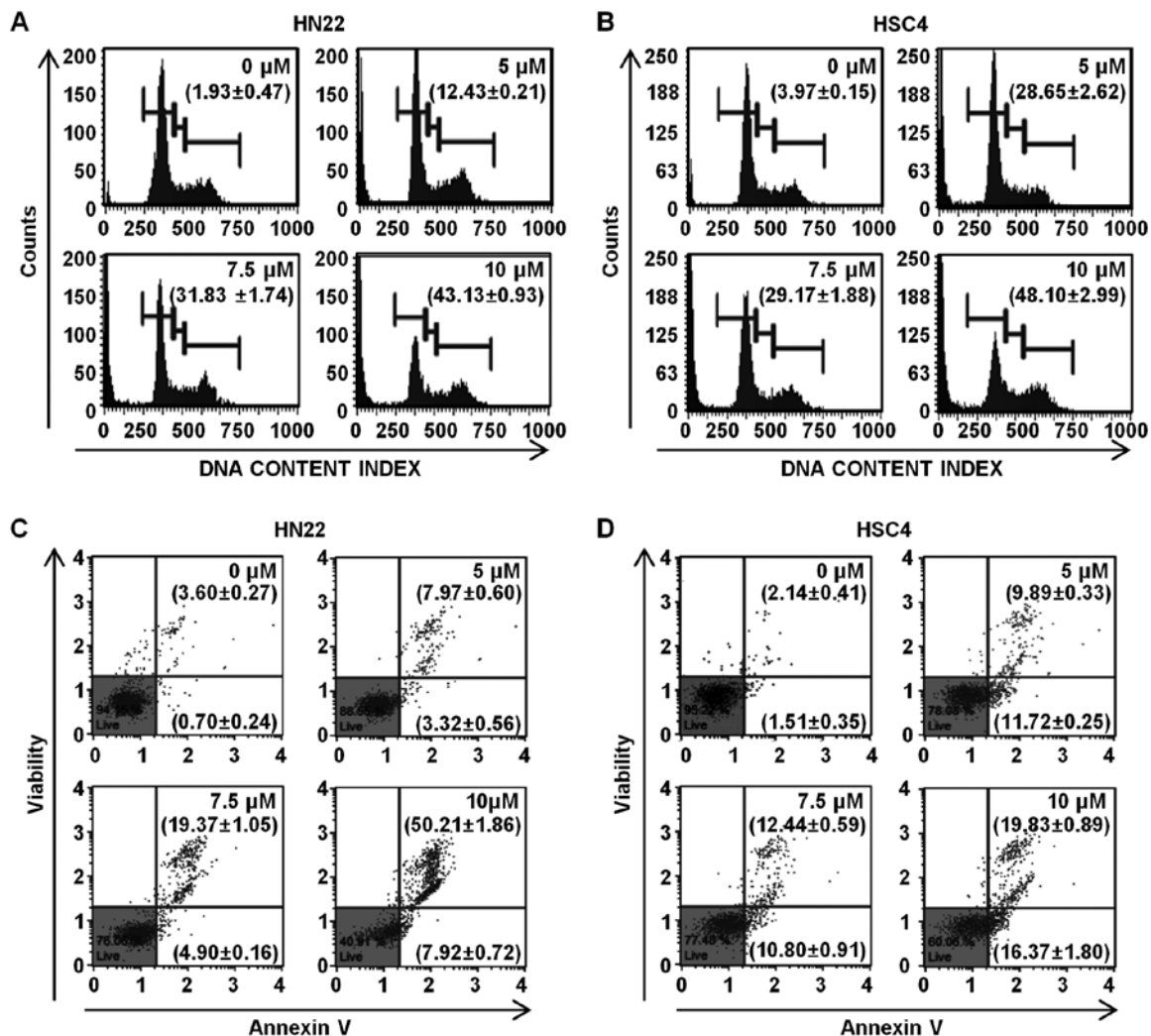


Figure 2. Effects of oridonin (Ordn) on cell cycle distribution and apoptosis of oral cancer cells. HN22 and HSC4 cells were treated with Ordn (0, 5, 7.5 and 10 μ M) for 48 h. (A) HN22 and (B) HSC4 cells were stained with Muse™ Cell Cycle Reagent. The percentage of oral cancer cells in the G0/G1, S and G2/M phases was calculated using the Muse™ cell analyzer. The sub-G1 percentages are written in the upper-right part of each graph. (C and D) Flow cytometric analysis demonstrates the proportion of total apoptotic cells. The analysis was based on binding activity of Annexin V in x-axis and the intensity of the 7-AAD fluorescence in y-axis. The cells can be classified into 4 categories: Live cells (lower-left quadrant), early apoptosis cell (lower-right quadrant), late apoptosis/dead cell (upper-right quadrant) and dead cell (upper-left quadrant). The data are representative of experiment 3 times and each time collected in triplicate. The data are the means \pm SD. * P <0.05 compared to the untreated group.

morphological changes, such as cell shrinkage, floating and large intercellular spacing. Ordn markedly suppressed colony formation in both the HN22 and HSC4 cells in a concentration-dependent manner (Fig. 1F and G). Ordn (2 μ M) inhibited colony formation by 48 and 43.14% in the HN22 and HSC4 cells, respectively.

Ordn induces the apoptosis of HN22 and HSC4 cells. To investigate chromatin condensation, fragmented nuclei and nuclear shrinkage, the nuclei of the Ordn-treated cells were observed after DAPI staining. The DAPI-stained nuclei of the HN22 and HSC4 cells were observed using fluorescence microscopy. The DAPI-stained cells were quantified and the apoptotic cell numbers were assessed as means with standard deviation by the graph. The results revealed apoptotic nuclei in the HN22 and HSC4 cells following Ordn treatment at concentrations of 5, 7.5 and 10 μ M for 48 h. The percentage of apoptosis was increased to 9.34, 24.44 and 43.18% in the HN22 cells and 10.83, 26.58 and 50.71% in the HSC4 cells with the

increasing concentrations of Ordn at 5, 7.5 and 10 μ M, respectively (Fig. 1E). To investigate the mechanisms responsible for Ordn-induced apoptosis, the HN22 and HSC4 cells were examined using the Cell Cycle kit and Annexin V and Dead cell kit in Muse™ cell analyzer. The HN22 and HSC4 cells were treated with 0, 5, 7.5 and 10 μ M Ordn for 48 h. We found that Ordn resulted in a significant concentration-dependent cell cycle arrest in the sub-G1 phase. The cell cycle distribution in the sub-G1 phase was 1.93 \pm 0.47, 12.43 \pm 0.21, 31.83 \pm 1.74 and 43.13 \pm 0.93% in the HN22 cells treated with Ordn at 0, 5, 7.5 and 10 μ M, respectively (Fig. 2A). The sub-G1 phase distribution in the HSC4 cells was 3.97 \pm 0.15, 28.65 \pm 2.62, 29.17 \pm 1.88 and 48.10 \pm 2.99% in the cells treated with Ordn at 0, 5, 7.5 and 10 μ M, respectively (Fig. 2B). To examine cell apoptosis, untreated or Ordn-treated HN22 and HSC4 cells were stained with Annexin V/7-AAD. As shown in Fig. 2C and D, treatment of the cells with Ordn at various concentrations (0, 5, 7.5 and 10 μ M) resulted in a dose-dependent increase in the early and late apoptotic population (4.3 \pm 0.4, 11.29 \pm 0.13, 24.27 \pm 0.99 and

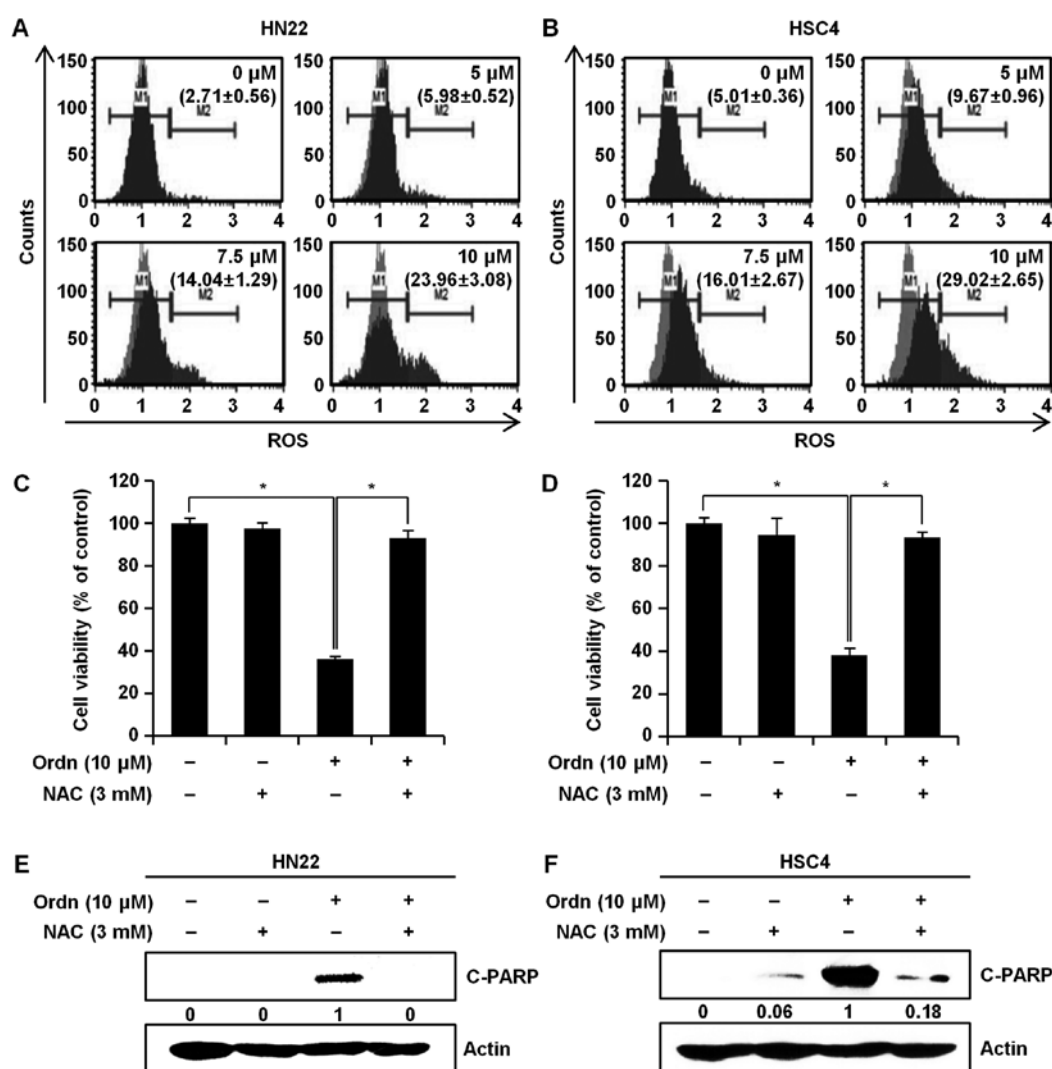


Figure 3. Apoptotic effects of oridonin (Ordn) are mediated through the generation of reactive oxygen species (ROS). HN22 and HSC4 cells were treated with Ordn at the indicated concentrations with or without NAC (3 mM) for 48 h and then (A and B) ROS assay, (C and D) MTT assay and (E and F) western blot analyses were carried out. (A and B) The levels of ROS were determined using the Muse™ cell analyzer. Cells in the M1 represent cells with a low fluorescence intensity, while cells in the M2 phase represent the population of ROS-positive cells. Data are presented as the means ± SD, n=3, *P<0.05. Cell lysates were subjected to western blot analysis with anti-cleaved PARP (C-PARP) and β-actin antibodies.

58.13±1.88% in the HN22 cells, and 3.65±0.06, 21.61±0.55, 23.24±1.47 and 36.2±2.64% in the HSC4 cells).

Ordn increases ROS generation. As reported previously, the increased generation of ROS can induce cell apoptosis (12,29). Thus, we measured the intracellular ROS levels using the Muse™ cell analyzer with the Muse™ Oxidative Stress kit. As shown in Fig. 3A and B, a marked increase in ROS levels was observed in the cells treated with Ordn at 0, 5, 7.5 and 10 μM for 48 h. In the HN22 cells, we observed a significant increase in ROS production, of 2.71±0.56, 5.98±0.52, 14.04±1.29 and 23.96±3.08% (M2 phase of ROS positively stained cells) at Ordn concentrations of 0, 5, 7.5 and 10 μM, respectively (Fig. 3A). For the HSC4 cells, the obtained results were 5.01±0.36, 9.67±0.96, 16.01±2.67 and 29.02±2.65% of the M2 phase cells, respectively (Fig. 3B). We then examined the protective effects of NAC in the Ordn-treated HN22 and HSC4 cells. NAC is widely used as a free radical scavenger (30). The cells were pretreated with 3 mM

NAC, followed by the addition of Ordn at 10 μM for 48 h. As shown in Fig. 3C and D, the loss of cell viability induced by Ordn was prevented by NAC. Moreover, western blot analysis of the HN22 and HSC4 cells revealed that Ordn enhanced the cleavage of PARP; however, pretreatment with NAC reversed these effects (Fig. 3E and F).

Ordn induces the apoptosis of oral cancer cells via the ROS-related p38 and JNK pathways. The MAPK pathways are one of the numerous cascades downstream of the ROS signaling pathway closely associated with apoptosis, as previously reported (31). In this study, we carried out western blot analysis to determine whether Ordn can induce the activation of the MAPK signaling pathway. Therefore, we examined the changes in the expression of proteins associated with the MAPK pathway, including p38 and JNK in the oral cancer cells following treatment with Ordn. The phosphorylation levels of p38 and JNK were markedly increased in response to Ordn treatment in the HN22 and HSC4 cells (Fig. 4).

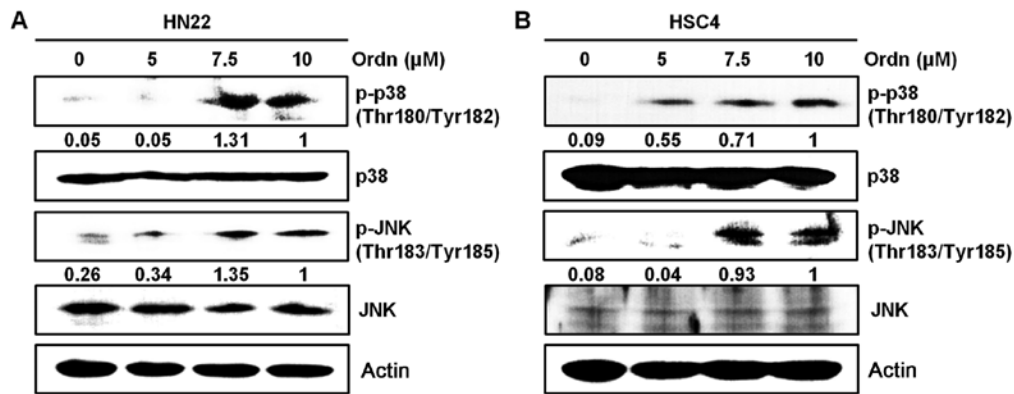


Figure 4. Activation of cell signaling proteins in (A) HN22 and (B) HSC4 cells following treatment with oridonin (Ordn). The oral cancer cells were treated with the indicated concentrations of Ordn (0, 5, 7.5 and 10 μ M) and western blot analysis was performed. The data were quantified using ImageJ software. p-p38 (Thr180/Tyr182) and p-JNK (Thr183/Tyr185) were normalized to the density of p38 and JNK, respectively.

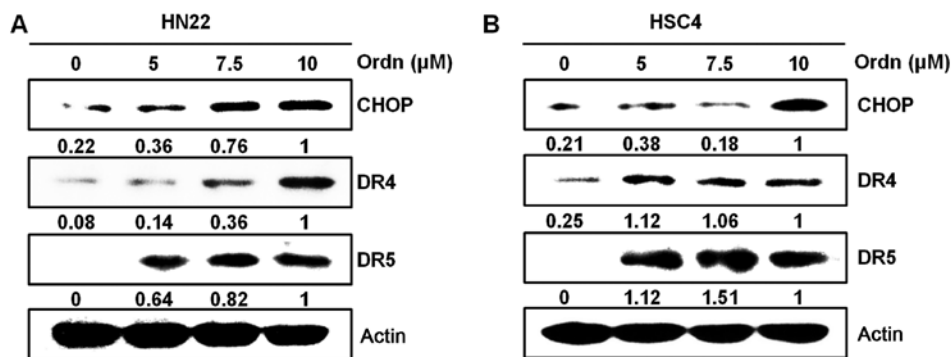


Figure 5. Effects of oridonin (Ordn) on endoplasmic reticulum (ER)-stress proteins. The (A) HN22 and (B) HSC4 cells were treated with Ordn (0, 5, 7.5 and 10 μ M) for 48 h. CHOP, DR4 and DR5 expression levels were determined by western blot analysis using specific antibodies. The specific bands were determined using ImageJ software. The protein expression levels were then normalized to actin.

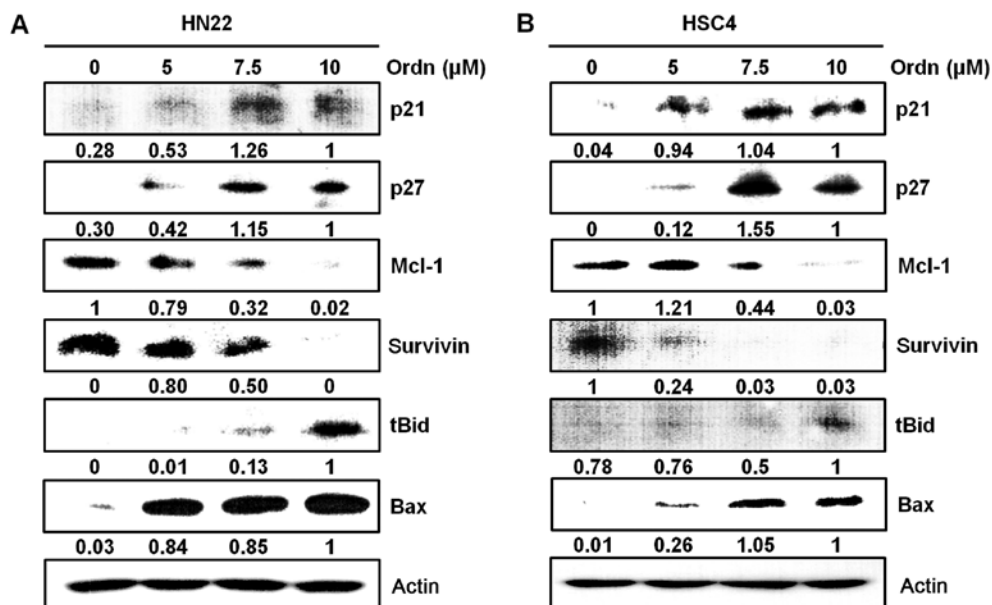


Figure 6. Effects of oridonin (Ordn) on p21, p27, Mcl-1, survivin, tBid and Bax expression. The (A) HN22 and (B) HSC4 oral cancer cells were treated with Ordn for 48 h. Proteins of interest in the cell lysates were detected using specific target antibodies. The blots were also examined with an anti- β -actin antibody to confirm equal loading of samples. Values were normalized against the relative expression of actin, determined using ImageJ software.

Ordn regulates the factors related to the apoptosis of oral cancer cells. A previous study provided evidence that ROS generation

is increased in ER stress (32). In addition, a close association has been identified between DR4 and DR5 expression and ER

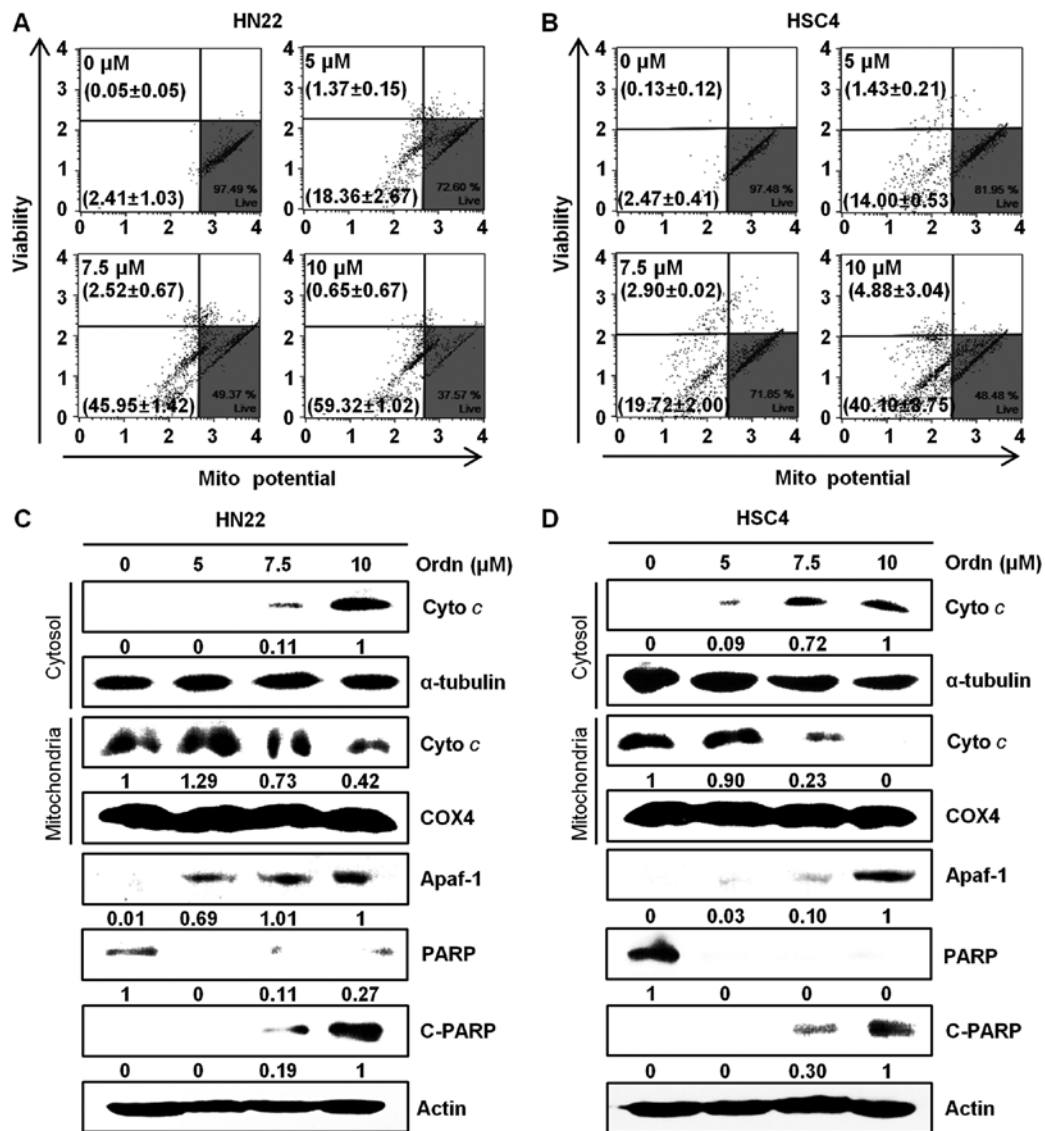


Figure 7. Effects of oridonin (Ordn) on mitochondrial membrane permeability. The cells were treated with 0, 5, 7.5 and 10 μ M of Ordn for 48 h. (A and B) Mitochondrial membrane potential (MMP) was measured using the Muse™ cell analyzer. The movement of the cell population from the right quadrant to the left quadrant indicates the depolarization of MMP, which is associated with the early stages of apoptosis. The results represent the means \pm SD of triplicate experiments. (C and D) Cyto *c* in the cytosolic and mitochondrial fraction was assessed by western blot analysis. The protein expression of Apaf-1, PARP and cleaved PARP (C-PARP) was also visualized by western blot analysis. The above proteins were quantified by ImageJ Instrument software. α -tubulin and COX4 were used as the controls for equal loading and fractionation quality. Apaf-1, PARP and C-PARP were normalized to the density of actin.

stress (20). As CHOP is an ER stress-inducible transcription factor (20), in this study, we examined whether Ordn treatment induces ER stress in the HN22 and HSC4 cells. Using western blot analysis, we examined whether the CHOP, DR4 and DR5 protein levels were upregulated following treatment of the cells with Ordn. Ordn treatment increased CHOP levels in the oral cancer cells, preceding the upregulation of the DR4 and DR5 levels (Fig. 5). To further characterize the molecular mechanisms responsible for Ordn-induced apoptosis, the expression levels of cell cycle modulators (p21 and p27), pro-apoptotic proteins (tBid and Bax) and anti-apoptotic proteins (Mcl-1 and survivin) were detected in the HN22 and HSC4 cells treated with Ordn. We found that Ordn decreased the expression of Mcl-1 and survivin, and increased p21, p27, tBid and Bax expression (Fig. 6). The Loss of mitochondrial inner transmembrane potential is a reliable indicator of mitochondrial dysfunction (21). This phenomenon is associated with the early

stages of apoptosis (33). In this study, following treatment of the cells with Ordn, the state of mitochondrial membranes was assessed using a Muse™ cell analyzer. Due to the accumulated fluorescent dye within inner membrane of intact mitochondria, control cells emit a high fluorescence intensity (34). Treatment of the cells with Ordn at a high concentration led to a decrease in fluorescence. Following treatment with Ordn at concentrations of 0, 5, 7.5 and 10 μ M, the percentage of depolarized HN22 cells was 2.41 ± 1.03 , 18.36 ± 2.67 , 45.95 ± 1.42 and $59.32 \pm 1.02\%$, respectively (Fig. 7A). The HSC4 cells exhibited a depolarized population of 2.47 ± 0.41 , 14.00 ± 0.53 , 19.72 ± 2.00 and $40.10 \pm 8.75\%$ at concentrations of 0, 5, 7.5 and 10 μ M Ordn, respectively (Fig. 7B). Furthermore, we examined the changes in the expression of downstream molecules that can occur after the loss of MMP. Firstly, we analyzed the release of cyto *c* as an apoptosis-related mitochondrial downstream molecule by western blot analysis. The cyto *c* protein is the pro-apoptotic

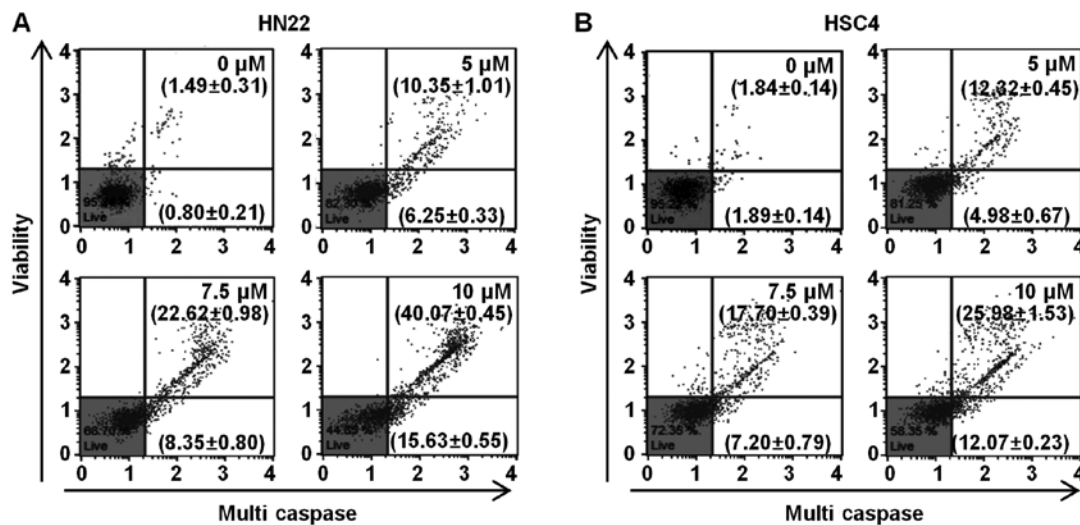


Figure 8. Effects of Ord on multi-caspase activity. The (A) HN22 and (B) HSC4 cells were treated with Ord at the indicated concentrations for 48 h. The fluorescence intensity of multiple caspases (caspase-1, -3, -4, -5, -6, -7, -8 and -9) was evaluated using the Muse™ cell analyzer. Ord induced the activation of several caspases in the oral cancer cells. Each quadrant indicates a population of viable cells (lower-left quadrant), cell population with caspase activity (lower-right quadrant), late stages including caspase activity/dead cells (upper-right quadrant) and dead cells (upper-left quadrant) in each experimental group. Results represent the means \pm SD from triplicate experiments.

mitochondrial protein located in the intermembrane space (35). Our data indicated that the amount of cyto *c* in the cytoplasm increased as a result of mitochondrial release in the HN22 and HSC4 cells treated with Ord (Fig. 7C and D). During the apoptotic cascades, Apaf-1 and PARP play an important role (35). Thus, in this study, the expression levels of Apaf-1, PARP and cleaved PARP in the oral cancer cells treated with Ord were examined by western blot analysis. As shown in Fig. 7C and D, the expression levels of Apaf-1 and cleaved PARP were increased significantly, whereas the expression of PARP was decreased in the HN22 and HSC4 cells treated with Ord. These results indicated that Ord regulated these proteins in a concentration-dependent manner. It is well known that the release of cyto *c* from the mitochondria can trigger a cascade of caspases, which is associated with the final pathway of cell apoptosis (36). The Muse™ Multi-Caspase assay kit was used to detect the presence of multiple caspases (caspase-1, -3, -4, -5, -6, -7, -8 and -9) apart from caspase-2. To determine whether caspase plays a role in the Ord-mediated apoptosis of oral cancer cells, the HN22 and HSC4 cells were examined using the Muse™ cell analyzer after Muse™ Multi-Caspase Reagent and Muse™ Caspase 7-AAD staining. The number represents the percentage of cells with caspase activity (lower right quadrant), and cell population of caspase activity/dead cells (upper right quadrant) in each condition. Multi-caspase activity was activated in the HN22 and HSC4 cells depending on the concentration of Ord (Fig. 8). The results indicated that the apoptosis of oral cancer cells was induced by Ord via the activation of caspases.

Discussion

The majority of patients with oral cancer have a high 5-year survival rate if the disease is detected in its earliest stage (37). Generally, various targets, such as cyclooxygenase and epidermal growth factor receptor have been suggested; however, oral cancer still has no specific target molecule (4).

Currently, anticancer drugs used in the treatment of oral cancer are highly toxic (6). Therefore, further research and the development of specific tumor biomarkers is warranted in order to enhance the efficacy of oral cancer treatment. It has been reported that Ord has an anti-inflammatory activity (8). Thus, in this study, we examined the anticancer effects of Ord on HN22 and HSC4 oral cancer cells, and also aimed to elucidate the underlying mechanisms.

To assess the anticancer effects of Ord on the OSCC cells, we conducted MTT assay, which is widely used to detect cell number, proliferation, cell viability, cell survival and toxicity (38). We found that Ord significantly suppressed cell proliferation and the colony-forming ability of both the HN22 and HSC4 cells in a dose-dependent manner (Fig. 1). Cell viability was further confirmed, based on the changes in cell morphological features using a microscope (Fig. 1D). Additionally, cell apoptosis was further corroborated by DAPI staining, propidium iodide staining and Annexin V/7-AAD staining (Figs. 1E and 2). The growth inhibitory effects induced by Ord were associated with an increase in the sub-G1 apoptotic population in the HN22 and HSC4 cells. Additionally, it was suggested that Ord may be associated with an increase in sub-G1 apoptotic population of OSCC cells through the p21 and p27 pathways, as Ord increased the expression of p21 and p27, which are cell cycle regulatory proteins (Fig. 6). Apoptosis is mediated in an orchestrated manner by two major pathways that is mediated by death receptors on the cell surface (extrinsic), and by mitochondria (intrinsic) (39). Due to the translocation of plasma membrane phosphatidylserine to the cell surface outer leaflet, apoptotic cells can be identified via the binding of Annexin V, which has a high affinity for phosphatidylserine (40). Furthermore, 7-AAD, a fluorescent DNA-binding agent, can discriminate the cells that are alive, dead, or in the early or late stages of apoptosis (41). In this study, the oral cancer cells treated with Ord were found to become Annexin V-positive in a dose-dependent manner, as shown by the rightward movement of the scatter plot compared with the

control cells (Fig. 2C and D). Thus, Ord_n can effectively induce the apoptosis of HN22 and HSC4 cells. It has been reported that CHOP directly regulates DR4 and DR5 expression during cell apoptosis to link between ER stress and DR5 expression (20). CHOP upregulation precedes the increase in DR4 and DR5 levels (42). In the present study, it was demonstrated that treatment of the oral cancer cells with Ord_n induced the expression of CHOP, DR4 and DR5 (Fig. 5). We provided some evidence that Ord_n triggers ER stress. A number of mechanisms have been proposed to explain ROS-mediated apoptosis and MAPK activation (15). ROS are responsible for the activation of the JNK and p38 pathways, and consequently lead to an increase in the levels of other pro-apoptotic molecules in cells (43). In this study, we evaluated whether Ord_n triggers intracellular ROS production and examined whether ROS mediate JNK and p38 MAPK signaling. Our results were quantitatively detected by MUSE™ to measure intracellular ROS levels. We found that Ord_n led to a significant increase in ROS levels in a concentration-dependent manner (Fig. 3A and B). To verify the direct effects of Ord_n-induced ROS production during cell apoptosis, we pretreated the cells with NAC, a ROS scavenger (44), prior to Ord_n treatment. As shown in Fig. 3C and D, pretreatment of the cells with NAC significantly suppressed Ord_n-induced apoptosis. In addition, NAC attenuated the activation of the cleavage of PARP (Fig. 3E and F). These findings indicate that ROS play an important role in Ord_n-induced oral cancer cell apoptosis.

The MAPK signaling pathways are composed of several sub-families of kinases, including p38, JNK (16). The sub-families have been greatly implicated in controlling cell proliferation, differentiation and apoptosis (15). In this study, to examine whether MAPK pathways are involved in Ord_n-induced apoptosis, we examined the activation of several protein kinases. It was found that Ord_n induced the phosphorylation of p38 and JNK (Fig. 4). The results demonstrated that Ord_n-induced apoptosis probably occurs through the regulation of p38 and JNK signaling pathways in the HN22 and HSC4 cells. Ord_n also altered the expression of specific pro-apoptotic/anti-apoptotic targets, such as tBid, Bax, Mcl-1 and survivin which are implicated in the apoptotic response (Fig. 6). Indeed, mitochondria metabolic pathways play crucial roles in cell apoptosis (18). MMP is crucial for the proton gradient across the mitochondria membrane and is lost due to the opening of the mitochondrial permeability transition pore (21). The depolarization of the mitochondrial membranes may lead to severe consequences, including a decrease in ATP synthesis and the redistribution of pro-apoptotic mitochondrial factors (21). The results of this study indicated that Ord_n induced a dose-dependent collapse of MMP in both the HN22 and HSC4 cells (Fig. 7A and B). The loss of mitochondrial transmembrane potential leads to the release of cyto *c* from the intermembrane space into the cytosol, suggesting the involvement of the mitochondrial pathway in cell apoptosis (22). In this study, Ord_n treatment led to cyto *c* release, which was confirmed by western blot analysis. In support of these findings, we observed that the release of cyto *c* into the cytosol was clearly associated with Apaf-1 and the cleavage of PARP (Fig. 7C and D). It is noteworthy that the upregulation of cleaved PARP was observed, as PARP was considered to be an important indicator of cell

apoptosis (45). The release of cyto *c* can lead to the activation of caspases, which are crucial effectors of apoptosis and the end-point features of apoptosis (22). Caspases are frequently associated with cleavage of a set of proteins, resulting in disassembly of the cell (25). In the present study, the sequential activation of multi-caspases was induced by Ord_n treatment, suggesting that caspases cascade functioned as crucial effectors for the triggering of apoptotic machinery by Ord_n in HN22 and HSC4 cells (Fig. 8).

In conclusion, it appears to be clear that Ord_n directly induces cell apoptosis probably through ROS generation and MAPK signaling pathways. These results further support the hypothesis that Ord_n exerts anticancer and antioxidant effects on oral cancer cells. Ord_n appears to be a promising drug candidate that can arrest the growth of oral cancer cells in the development of future anti-oral cancer treatments. Therefore, further studies using animal studies and clinical trials are warranted in order to evaluate and validate the anticancer effects of Ord_n.

Acknowledgements

Not applicable.

Funding

This study was supported by grants (16182MFDS391) from the Korean Ministry of Food and Drug Safety in 2017. This study was also carried out with the support of the 'Cooperative Research Program for Agriculture Science and Technology Development (Project no. PJ012704012018)' project of the National Institute of Animal Science, Rural Development Administration, Republic of Korea. This research was also supported by grants (81572812) from the National Natural Science Foundation of China.

Availability of data and materials

The analyzed datasets generated during the study are available from the corresponding author on reasonable request.

Authors' contributions

HNO, JHSe, JIC and JHSh contributed to the design of the study and wrote the manuscript. HNO, JHSe, MHL, GY, SSC, KL, HC, KBO, YSC, HK and ALH were responsible for data acquisition, data analysis and interpretation. HNO, JIC and JHSh were responsible for article revision. MHL, GY, SSC, KL, HC, KBO, YSC and HK were responsible for data interpretation and methodology. JIC and JHSh were responsible for funding acquisition and supervision. All authors have read and approved the final version of this manuscript.

Ethics approval and consent to participate

Not applicable.

Consent for publication

Not applicable.

Competing interests

The authors declare that they have no competing interests.

References

- Schneider K, Roller M, Kalberlah F and Schuhmacher-Wolz U: Cancer risk assessment for oral exposure to PAH mixtures. *J Appl Toxicol* 22: 73-83, 2002.
- Awan KH and Patil S: Association of smokeless tobacco with oral cancer - Evidence from the South Asian Studies: A Systematic Review. *J Coll Physicians Surg Pak* 26: 775-780, 2016.
- Chi AC, Day TA and Neville BW: Oral cavity and oropharyngeal squamous cell carcinoma - an update. *CA Cancer J Clin* 65: 401-421, 2015.
- Rivera C: Essentials of oral cancer. *Int J Clin Exp Pathol* 8: 11884-11894, 2015.
- Brocklehurst P, Kujan O, O'Malley LA, Ogden G, Shepherd S and Glenny AM: Screening programmes for the early detection and prevention of oral cancer. *Cochrane Database Syst Rev* 11: CD004150, 2013.
- Maggioni D, Biffi L, Nicolini G and Garavello W: Flavonoids in oral cancer prevention and therapy. *Eur J Cancer Prev* 24: 517-528, 2015.
- Kao J, Sikora AT and Fu S: Dual EGFR and COX-2 inhibition as a novel approach to targeting head and neck squamous cell carcinoma. *Curr Cancer Drug Targets* 9: 931-937, 2009.
- Zhao Z and Chen Y: Oridonin, a promising antitumor natural product in the chemotherapy of hematological malignancies. *Curr Pharm Biotechnol* 15: 1083-1092, 2014.
- Ding Y, Ding C, Ye N, Liu Z, Wold EA, Chen H, Wild C, Shen Q and Zhou J: Discovery and development of natural product oridonin-inspired anticancer agents. *Eur J Med Chem* 122: 102-117, 2016.
- Owona BA and Schluesener HJ: Molecular insight in the multifunctional effects of oridonin. *Drugs R D* 15: 233-244, 2015.
- Li D, Han T, Liao J, Hu X, Xu S, Tian K, Gu X, Cheng K, Li Z, Hua H, *et al*: Oridonin, a promising ent-Kaurane diterpenoid lead compound. *Int J Mol Sci* 17: 17, 2016.
- Schieber M and Chandel NS: ROS function in redox signaling and oxidative stress. *Curr Biol* 24: R453-R462, 2014.
- Kamogashira T, Fujimoto C and Yamasoba T: Reactive oxygen species, apoptosis, and mitochondrial dysfunction in hearing loss. *BioMed Res Int* 2015: 617207, 2015.
- Darling NJ and Cook SJ: The role of MAPK signalling pathways in the response to endoplasmic reticulum stress. *Biochim Biophys Acta* 1843: 2150-2163, 2014.
- Jalimi SK and Sinha AK: ROS mediated MAPK signaling in abiotic and biotic stress- striking similarities and differences. *Front Plant Sci* 6: 769, 2015.
- Huang G, Shi LZ and Chi H: Regulation of JNK and p38 MAPK in the immune system: Signal integration, propagation and termination. *Cytokine* 48: 161-169, 2009.
- Ouyang L, Shi Z, Zhao S, Wang FT, Zhou TT, Liu B and Bao JK: Programmed cell death pathways in cancer: A review of apoptosis, autophagy and programmed necrosis. *Cell Prolif* 45: 487-498, 2012.
- Elmore S: Apoptosis: A review of programmed cell death. *Toxicol Pathol* 35: 495-516, 2007.
- Urrea H, Dufey E, Lisbona F, Rojas-Rivera D and Hetz C: When ER stress reaches a dead end. *Biochim Biophys Acta* 1833: 3507-3517, 2013.
- Sano R and Reed JC: ER stress-induced cell death mechanisms. *Biochim Biophys Acta* 1833: 3460-3470, 2013.
- Kroemer G, Galluzzi L and Brenner C: Mitochondrial membrane permeabilization in cell death. *Physiol Rev* 87: 99-163, 2007.
- Tait SW and Green DR: Mitochondria and cell signalling. *J Cell Sci* 125: 807-815, 2012.
- Martinou JC and Youle RJ: Mitochondria in apoptosis: Bcl-2 family members and mitochondrial dynamics. *Dev Cell* 21: 92-101, 2011.
- Tsujimoto Y: Role of Bcl-2 family proteins in apoptosis: apoptosis or mitochondria? *Genes Cells* 3: 697-707, 1998.
- Fernald K and Kurokawa M: Evading apoptosis in cancer. *Trends Cell Biol* 23: 620-633, 2013.
- Cardinali M, Pietraszkiewicz H, Ensley JF and Robbins KC: Tyrosine phosphorylation as a marker for aberrantly regulated growth-promoting pathways in cell lines derived from head and neck malignancies. *Int J Cancer* 61: 98-103, 1995.
- Darzynkiewicz Z: Cytometry of the cell cycle: In search for perfect methodology for DNA content analysis in tissue specimens. *Cell Cycle* 9: 3395-3396, 2010.
- Twentyman PR and Luscombe M: A study of some variables in a tetrazolium dye (MTT) based assay for cell growth and chemosensitivity. *Br J Cancer* 56: 279-285, 1987.
- Jeong CH and Joo SH: Downregulation of reactive oxygen species in apoptosis. *J Cancer Prev* 21: 13-20, 2016.
- Sun SY: N-acetylcysteine, reactive oxygen species and beyond. *Cancer Biol Ther* 9: 109-110, 2010.
- Son Y, Cheong YK, Kim NH, Chung HT, Kang DG and Pae HO: Mitogen-activated protein kinases and reactive oxygen species: How can ROS activate MAPK pathways? *J Signal Transduct* 2011: 792639, 2011.
- Verfaillie T, Rubio N, Garg AD, Bultynck G, Rizzuto R, Decuyper JP, Piette J, Linehan C, Gupta S, Samali A, *et al*: PERK is required at the ER-mitochondrial contact sites to convey apoptosis after ROS-based ER stress. *Cell Death Differ* 19: 1880-1891, 2012.
- Castedo M, Ferri K, Roumier T, Métévier D, Zamzami N and Kroemer G: Quantitation of mitochondrial alterations associated with apoptosis. *J Immunol Methods* 265: 39-47, 2002.
- Poncet D, Boya P, Métévier D, Zamzami N and Kroemer G: Cytofluorometric quantitation of apoptosis-driven inner mitochondrial membrane permeabilization. *Apoptosis* 8: 521-530, 2003.
- Fan TJ, Han LH, Cong RS and Liang J: Caspase family proteases and apoptosis. *Acta Biochim Biophys Sin (Shanghai)* 37: 719-727, 2005.
- Monian P and Jiang X: Clearing the final hurdles to mitochondrial apoptosis: Regulation post cytochrome c release. *Exp Oncol* 34: 185-191, 2012.
- Montero PH and Patel SG: Cancer of the oral cavity. *Surg Oncol Clin N Am* 24: 491-508, 2015.
- Stockert JC, Blázquez-Castro A, Cañete M, Horobin RW and Villanueva A: MTT assay for cell viability: Intracellular localization of the formazan product is in lipid droplets. *Acta Histochem* 114: 785-796, 2012.
- Ilmarinen P, Moilanen E and Kankaanranta H: Mitochondria in the center of human eosinophil apoptosis and survival. *Int J Mol Sci* 15: 3952-3969, 2014.
- He Z, Sun Q, Liang YJ, Chen L, Ge YF, Yun SF and Yao B: Annexin A5 regulates Leydig cell testosterone production via ERK1/2 pathway. *Asian J Androl* 18: 456-461, 2016.
- Balmer J, Zulliger R, Roberti S and Enzmann V: Retinal cell death caused by sodium iodate involves multiple caspase-dependent and caspase-independent cell-death pathways. *Int J Mol Sci* 16: 15086-15103, 2015.
- Stolfi C, Pallone F and Monteleone G: Molecular targets of TRAIL-sensitizing agents in colorectal cancer. *Int J Mol Sci* 13: 7886-7901, 2012.
- Zhang J, Wang X, Vikash V, Ye Q, Wu D, Liu Y and Dong W: ROS and ROS-mediated cellular signaling. *Oxid Med Cell Longev* 2016: 4350965, 2016.
- Bjørn ME and Hasselbalch HC: The role of reactive oxygen species in myelofibrosis and related neoplasms. *Mediators Inflamm* 2015: 648090, 2015.
- Zhang F, Lau SS and Monks TJ: A dual role for poly(ADP-ribose) polymerase-1 during caspase-dependent apoptosis. *Toxicol Sci* 128: 103-114, 2012.